Epitaxial growth and dielectric properties of homologous $Sr_{m-3}Bi_4Ti_mO_{3m+3}$ (m=3,4,5,6) thin films

S. T. Zhang[a] and Y. F. Chen
Department of Materials Science and Engineering and National Laboratory of Solid State Microstructures, Nanjing University, Nanjing 210093, People's Republic of China

H. P. Sun and X. Q. Pan
Department of Materials Science and Engineering, The University of Michigan, Ann Arbor, Michigan 48109-2136

Z. G. Liu and N. B. Ming
Department of Materials Science and Engineering and National Laboratory of Solid State Microstructures, Nanjing University, Nanjing 210093, People's Republic of China

The first four members of Bi-layered $Sr_{m-3}Bi_4Ti_mO_{3m+3}$ homologous series with m=3, 4, 5, and 6, i.e., $Bi_4Ti_3O_{12}$, $SrBi_4Ti_4O_{15}$, $Sr_2Bi_4Ti_5O_{18}$, and $Sr_3Bi_4Ti_6O_{21}$, were grown on $SrTiO_3$ (001) single-crystal substrates by pulsed-laser deposition. X-ray diffraction and high-resolution transmission electron microscopy (HRTEM) reveal that the films grew epitaxially with in-plane epitaxial alignment of $[1\bar{1}0]Sr_{m-3}Bi_4Ti_mO_{3m+3}\|[010]SrTiO_3$. HRTEM cross-sectional images show that the films with m=3, 4, and 5 are nearly free of intergrowth, whereas a number of growth defects were observed in the film with m=6. Using an evanescent microwave probe, the room-temperature dielectric constants of these epitaxial films are measured to be 221 ± 13, 205 ± 15, 261 ± 29, and 249 ± 17 for films with m=3, 4, 5, and 6, respectively. © *2002 American Institute of Physics.* [DOI: 10.1063/1.1530741]

There has been a lot of interest in ferroelectric thin films since their unique dielectric, piezoelectric, pyroelectric, and ferroelectric properties can be utilized for memory devices, ultrasonic sensors, and infrared detectors.[1–3] In recent years, Bi-layered perovskites exemplified by $SrBi_2Ta_2O_9$ (SBT) thin films have been extensively studied for use in nonvolatile ferroelectric random access memories (NVFRAMs).[4,5] It is well known that these materials show highly anisotropic structure, ther fare, highly anisotropic ferroelectric properties. In view of applications in infrared detectors and NV-FRAMs, the growth of non-c-axis oriented films is of particular significance because the direction of spontaneous polarization in these materials is perpendicular to the c axis, specifically along the a or b axis.[6–8] However, c-axis epitaxial SBT films have been confirmed to be useful high-k dielectric materials.[9] In addition, probing c-axis epitaxial films of these unconventional materials can reveal their basic structural and intrinsic properties.[10]

On the other hand, it was suggested that Bi-layered oxides with $m>5$ could not occur naturally and some attempts to fabricate such oxides ended up in a mixture of phases of $SBTi_5$ and $SrTiO_3$,[11] however, there is no direct reason to preclude their occurrence, especially in the form of thin films. In the case of $Sr_3Bi_4Ti_6O_{21}$, which should have six octahedral blocks between two neighboring $(Bi_2O_2)^{2+}$ layers, although its optical properties have been reported,[12] as far as we know no careful structural characterization [i.e., using a high-resolution transmission electron microscope (HRTEM)] of it has been done to ensure it is really a single

phase material. To resolve this, HRTEM studies of c-axis epitaxial $SBTi_6$ thin films are necessary.

The synthesis of homologous oxide thin film system can offer tremendous potential for tailoring the ferroelectric and dielectric properties of materials. For example, by preparing the first five members of the $Sr_{n+1}Ti_nO_{3n+1}$ Ruddlesden–Popper homologous series by molecular beam epitaxy (MBE), Haeni *et al.* revealed that the first member of this series, Sr_2TiO_4, has several potential advantages over the $n=\infty$ member, $SrTiO_3$, for application in metal–oxide–semiconductor field-effect transistors (MOSFETs).[13]

Motivated by the work described above, we prepared c-axis epitaxial homologous $Sr_{m-3}Bi_4Ti_mO_{3m+3}$ (m=3, 4, 5, and 6), i.e., $Bi_4Ti_3O_{12}$, $SrBi_4Ti_4O_{15}$, $Sr_2Bi_4Ti_5O_{18}$, and $Sr_3Bi_4Ti_6O_{21}$ (referred to as BTO, $SBTi_4$, $SBTi_5$, and $SBTi_6$, respectively) thin films on (001)-$SrTiO_3$ (STO) single-crystal substrates by pulsed laser deposition (PLD) and studied their dielectric properties. These materials belong to the family of Bi-layered perovskite oxides with 3, 4, 5, and 6 TiO_6 octahedra sandwiched between two neighboring $(Bi_2O_2)^{2+}$ layers. Corresponding schematics representations of the crystal structures of these materials are shown in Figs. 1(a)–1(d).

According to *Hesse et al.*,[14] for Bi-layered oxides, a pseudotetragonal or orthorhombic structure can be used. In the case of the pseudotetragonal structure, the a- and b-lattice constants of these materials are about 3.84–3.86 Å, which show little variation with respect to the m value and are very similar to the lattice constant of cubic STO (a=3.90 Å) and that of pseudocubic LaAlO$_3$ (LAO, a=3.79 Å). The lattice mismatches of these materials between STO are less than 1.54% and between LAO are less than 1.32%, therefore,
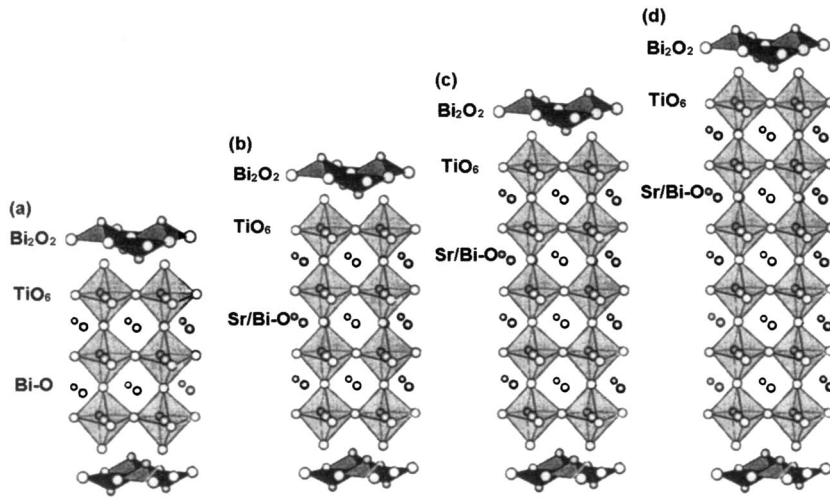
FIG. 1. Schematics of the crystal structure of (a) BTO, (b) $SBTi_4$, (c) $SBTi_5$, and (d) $SBTi_6$.

STO and LAO might be promising as substrates for the growth of *c*-axis epitaxial $Sr_{m-3}Bi_4Ti_mO_{3m+3}$ ($m=3$, 4, 5, and 6) thin films. In this letter, however, orthorhombic structure indexing will be used.

Ceramic pellets used as PLD targets were prepared by a citrate complex method and a solid-state reaction method. The PLD processes were performed using a KrF excimer laser with wavelength of 248 nm and pulse width of 30 ns. Details of the preparation procedures will be given later.

The crystal structures and epitaxial arrangements of the films were studied by x-ray diffraction (XRD) using a Rigaku-D/Max-rA diffractometer with Cu $K\alpha$ radiation and by HRTEM using a JEOL 4000EX electron microscope operating at 400 kV, which provided a point resolution of 1.7 nm. Dielectric constants at room temperature were measured using an evanescent microwave probe (EMP).[13,15,16]

The θ–2θ XRD patterns of the BTO, $SBTi_4$, $SBTi_5$, and $SBTi_6$ films fabricated on (001)-STO substrates are shown in Figs. 2(a)–2(d). The peaks of BTO, $SBTi_4$, and $SBTi_5$ were indexed according to standard powder diffraction data whereas the peaks of $SBTi_6$ were indexed by assuming $c = 5.700$ nm.[12] It should be noted that standard powder diffraction data of $Pb_3Bi_4Ti_6O_{21}$[17] are a valuable reference for indexing the peaks of $SBTi_6$ films. Obviously, only $(002l)$ peaks of these materials and $(00l)$ peaks of STO substrates can be detected, consistent with in other reports.[9,12] The space groups of the Bi-layered Aurivillius phases are $A2_1am$ for even m_l and $B2_1bm$ for odd m. Both have glide planes along the c axis,[18] which could be responsible for the extinction of $(0\,0\,2l+1)$ peaks. However, local structural distortion might result in weak $(0\,0\,2l+1)$ peaks.

Figure 3(a) is a low magnification TEM micrograph of a cross-sectional sample that shows the morphology of the $SBTi_4$ film on STO. A columnar structure consisting of a subgrain boundary can be seen. The film consists of a sharp interface with respect to the substrate and has a mean thickness of 735 nm. Figure 3(b) shows a typical [010] zone axis selected-area electron diffraction (SAED) pattern of the STO
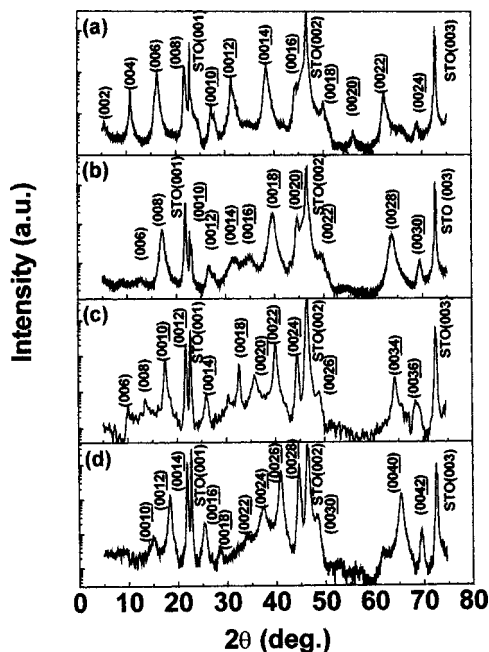

FIG. 2. X-ray θ–2θ scans of (a) BTO, (b) $SBTi_4$, (c) $SBTi_5$, and (d) $SBTi_6$ films grown on (001)-STO single-crystal substrates.
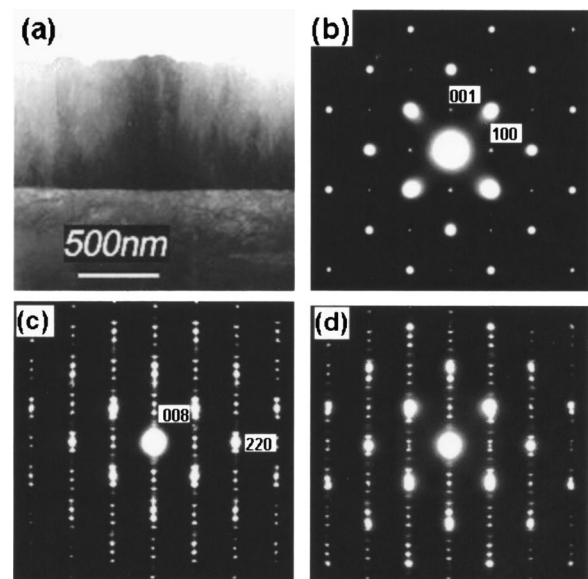

FIG. 3. (a) Cross-sectional TEM micrograph of $SBTi_4$ film grown on a (001)-STO substrate and typical SAED patterns of (b) the [010] zone of STO, (c) the [$1\bar{1}0$] zone of $SBTi_4$, and (d) the interface between STO and $SBTi_4$.
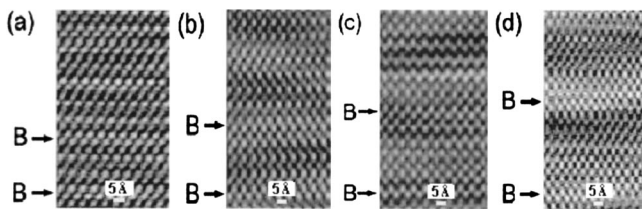
FIG. 4. Cross-sectional HRTEM images of (a) BTO, (b) $SBTi_4$, (c) $SBTi_5$, and (d) $SBTi_6$ films. B indicates $(Bi_2O_2)^{2+}$ layers.

substrate. Figures 3(c) and 3(d) are SAED patterns taken of the $SBTi_4$ films and of the interface between $SBTi_4$ films and the STO substrate. Figure 3(c) is the $[1\bar{1}0]$ zone electron diffraction pattern of the $SBTi_4$ structure. Note that orthorhombic indexing is used. Clearly, Fig. 3(d) shows the mixing of $[010]$STO and $[1\bar{1}0]SBTi_4$ in the SAED pattern. For BTO, $SBTi_5$, and $SBTi_6$ films on (001)-STO substrates, similar cross-sectional TEM morphologies (thicknesses of 452, 432, and 500 nm, respectively) and SAED patterns are also obtained. From these SAED patterns, the following epitaxial relation is established: $(001)Sr_{m-3}Bi_4Ti_mO_{3m+3}\parallel$ $(001)SrTiO_3$ and $[1\bar{1}0]Sr_{m-3}Bi_4Ti_mO_{3m+3}\parallel[010]SrTiO_3$. X-ray ϕ scans of the (117), (119), (1111), and (1113) peaks of the $m=3-6$ phases, respectively, also indicate the same epitaxial relation.

Figures 4(a)–4(d) present cross-sectional HRTEM images of the *c*-axis epitaxial BTO, $SBTi_4$, $SBTi_5$, and $SBTi_6$ films. The spots corresponding to the Sr and Ti columns have relatively low intensity, the Bi columns high intensity, and the O columns are not seen. This is because of the different atomic numbers, $Z=38$, 22, 83, and 8, for Sr, Ti, Bi, and O, respectively. The Sr and Ti columns have little difference in intensity because of the closeness of their atomic numbers. For each material, the stacking blocks of the alternate Bi_2O_2 layers and TiO_6 octahedra can be identified. The Bi_2O_2 layers are indicated by B; the TiO_6 octahedra lie between two neighboring $(Bi_2O_2)^{2+}$ layers, which fit the schematic of the crystal structure shown in Fig. 1 well. The equal spacing between the double Bi_2O_2 layers indicates a single-phase film. It should be noted that between double Bi_2O_2 layers, there are other Bi columns that can be detected, and they correspond to Bi–Ti–O ferroelectric blocks. The measured *c*-axis lattice constants of $m=3-6$ films are 32.8, 40.4, 49.1, and 56.7 Å. No intergrowth is observed in the imaged area of the $m=3$, 4 and 5 films. However, some intergrowth of $m=6$ phase is observed in the localized region. In addition, a distorted line can be seen in the $m=5$ and 6 phases. It is reported that TiO_6 octahedra can tilt along the four nominally equivalent *a* axes;[19] this tilting will lead to atoms such as Ti bending upward or downward to the left or right irrationally. A repeated small bend will form this type of distorted line.

Growth of the *c*-axis epitaxial films allows the ε_{33} dielectric constants of these high anisotropic materials to be measured. The room-temperature dielectric constants (ε_r) of these films were measured with the EMP. The films mea-sured with the EMP were grown directly on (001)-LAO single-crystal substrates by PLD. LAO was used as the substrate instead of STO because its low dielectric constant ($\sim$24) will not interfere with the dielectric measurement. The measured ε_r are 221 ± 13, 205 ± 15, 261 ± 29, and 249 ± 17 for $m=3$, 4, 5, and 6 films, respectively. These are comparable in magnitude to the results measured in the parallel plate capacitor structure $(LaNiO_3/Sr_{m-3}Bi_4Ti_mO_{3m+3}/$ $LaNiO_3/LaAlO_3$ with $m=3-6$) with a HP4294A impedance/phase analyzer.

In conclusion, epitaxial BTO, $SBTi_4$, $SBTi_5$, and $SBTi_6$ films were prepared on (100)-STO single-crystal substrates by PLD. Cross-sectional HRTEM and electron diffraction studies revealed that the films have single phases. Octahedral tilting of these Bi-layered perovskite oxides was observed. The dielectric measurements revealed that these films showed high dielectric constants.

[1] J. F. Scott and C. A. P. de Araujo, Science **246**, 1400 (1989).
[2] K. Lijima, Y. Tomita, R. Takeyama, and I. Ueda, J. Appl. Phys. **60**, 361 (1990).
[3] M. H. Francombe and S. V. Krinnawamy, J. Vac. Sci. Technol. A **8**, 1382 (1990).
[4] C. A. P. de Araujo, J. D. Cuchiaro, L. D. McMillan, M. C. Scott, and J. F. Scott, Nature (London) **374**, 12 (1995).
[5] B. H. Park, B. S. Kang, S. D. Bu, T. W. Noh, J. Lee, and W. Jo, Nature (London) **401**, 682 (1999).
[6] J. Lettieri, M. A. Zurbuchen, Y. Jia, D. G. Schlom, S. K. Streiffer, and M. E. Hawley, J. Appl. Phys. **76**, 2937 (2000).
[7] R. L. Withers, J. G. Thompson, and A. D. Rae, J. Solid State Chem. **94**, 404 (1991).
[8] K. M. Satyalakshmi, M. Alexe, A. Pignolet, N. D. Zakharov, C. Harnagea, S. Senz, and D. Hesse, Appl. Phys. Lett. **74**, 603 (1999).
[9] S. Chattopadhyay, A. Kvit, D. Kumar, A. K. Sharma, J. Sankar, J. Narayan, V. S. Knight, T. S. Coleman, and C. B. Lee, Appl. Phys. Lett. **78**, 3514 (2001).
[10] Y. Yan, M. M. Al-Jassim, Z. Xu, X. Lu, D. Viehland, M. Payne, and S. J. Pennycook, Appl. Phys. Lett. **75**, 1961 (1999).
[11] B. Aurivillius and P. H. Fang, Phys. Rev. **126**, 893 (1962).
[12] M. Tachiki, K. Yamamuro, and T. Kobayashi, Jpn. J. Appl. Phys., Part 2 **35**, L719 (1996).
[13] J. H. Haeni, C. D. Theis, D. G. Schlom, W. Tian, X. Q. Pan, H. Chang, I. Takeuchi, and X. D. Xiang, Appl. Phys. Lett. **78**, 3292 (2001).
[14] D. Hesse, N. D. Zakharov, A. Pignolet, A. R. James, and S. Senz, Cryst. Res. Technol. **35**, 641 (2000).
[15] C. Gao and X.-D. Xiang, Rev. Sci. Instrum. **69**, 3846 (1998).
[16] H. Chang, I. Takeuchi, and X.-D. Xiang, Appl. Phys. Lett. **74**, 1165 (1999).
[17] T. Kikuchi, MRS Bull. **14**, 1561 (1979).
[18] A. D. Rae, J. G. Thompson, R. L. Withers, and A. C. Willis, Acta Crystallogr., Sect. B: Struct. Sci. **B46**, 474 (1990).
[19] D. J. Srolovitz and J. F. Scott, Phys. Rev. B **34**, 1815 (1986).